Control of Grid Connected PV Cell Distributed Generation Systems

J.Nagarjuna Reddy, M.Kalia Moorthy*, D.V. Ashok Kumar**

Assistant Professor, Dept. of EEE, RGMCET, Nandyal, India, nagarjunamtech@gmail.com
*Associate Professor, Dept. of EEE, PSNA CET, Dindugal, India, kalias_ifet@yahoo.com
**Professor, Dept. of EEE, RGMCET, Nandyal, India, dvakdl@gmail.com

***Abstract*-This paper presents modeling, controller design, and simulation study of a grid connected Photovoltaic (GCPV) distributed generation (DG) system. The overall configuration of the grid connected photovoltaic DG system are present. The dynamic models for the GCPV power plant and its power electronic interfacing are described. Controller design methodologies for the control of power flow from the photovoltaic cell power plant to the utility grid are also presented. A Matlab/Simulink based simulation model is developed for the GCPV DG system by combining the individual component models and the controllers design. Simulation results are presented to show the overall system performance.**

***Keywords*--Control, distributed generation (DG), interfacing, modeling, Grid connected photovoltaic (GCPV)**

I. INTRODUCTION

The Ever-Increasing energy consumption and the rising public awareness for environmental protection have created increased interest in green (i.e., renewable and photovoltaic based) power generation systems. Moreover, due to steady progress in power deregulation, utility restructuring and because of tight constraints are imposed on the construction of new transmission lines for long-distance power transmission, interest in distributed generation (DG) systems installed near load centers is increasing.

Photovoltaic cells are static energy conversion devices that convert the solar energy directly into electrical energy. They shows great promise to be an important DG source of the future due to their many advantages, such as high efficiency, zero or low emission (of pollutant gases), and flexible modular structure. Grid connected PV systems have become one of the important applications of solar energy. Grid-connected PV plants makes good economic sense to maximize the amount of power generated by PV arrays and thus transferred to the grid at all times. An important technique for achieving the above is called the maximum power point tracking (MPPT). In principle, this controls the output of a PV system to match with the grid for all atmospheric conditions. Hence, it results in the system operating at the maximum power point at all times.

This paper presents the modeling and control of a GCPV system. The Photovoltaic cell power plant is interfaced with the utility grid via boost dc/dc converters and a three-phase pulse width modulated (PWM) inverter. A validated GCPV dynamic model, reported in [1] is used in this paper. The models for the boost dc/dc converter and the three-phase inverter together with an *LC* filter transmission lines are also addressed. The controller design methodologies for the dc/dc converter and the three-phase inverter are also presented for the proposed GCPV DG system. A neural network based MPPT algorithm is proposed in this paper. Based on the individual component models developed and the controller design, a simulation model of the GCPV DG system has been built in Matlab/Simulink.

II. SYSTEM DESCRIPTION

To meet the system operational requirements, a photovoltaic DG system needs to be interfaced through a set of power electronic devices. The interface is very important as it affects the operation of the PV cell system as well as the power grid. Pulse-width modulated voltage source inverters (VSI) is used to interconnect a PV system to a utility grid. In addition, PV systems normally need boost dc/dc converters to track the maximum output voltage, smooth PV output current to make the PV cell operate at maximum efficiency [1].

The schematic block diagram of a grid connected photovoltaic system proposed in this paper is as shown in Fig.1. For maximum utilization efficiency of a PV cell, it is necessary to operate the cell at maximum power point. But it is difficult to operate the cell at MPP always as it depends on the atmospheric conditions such as cell temperature and irradiance. Various methods to realize MPPT have been reported in the literature. The proposed neural network based MPPT is presents in this paper.

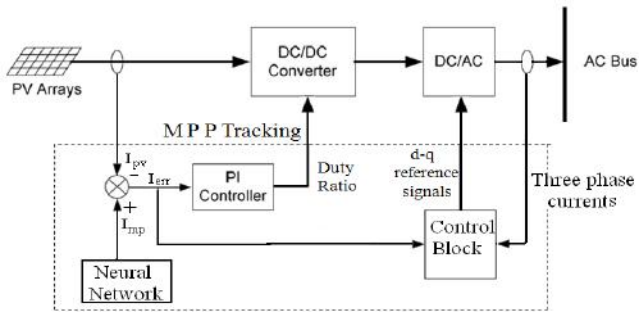

Fig.1.Block diagram of a grid connected photovoltaic system

A three-phase six switch inverter interfaces dc-dc boost converter with an a.c grid. A neural network based high performance current regulator combining with a space vector modulation PWM scheme has been used to control the inverter. Discussions of the method and simulation results are presented in the paper.

III. DYNAMIC MODELS FOR PV CELL AND POWER

This section describes the dynamic models for the main components of the system shown in Fig.1, namely for the PV array, Neural Network for MPPT, DC/DC Converter and the Three-phase inverter.

A. Dynamic Model for the Photovoltaic Cell

It is well known that a PV array consists of a collection of solar cells connected in series and/or parallel. Each of these cells is basically a p-n diode that convert the light energy into electrical energy. The most commonly used One-diode equivalent circuit models for a PV cell is as shown in Fig.2. Since the shunt resistance R_{sh} is large, it is normally neglected. This simplified circuit is used in this paper for modeling of a PV-cell [1]-[4].

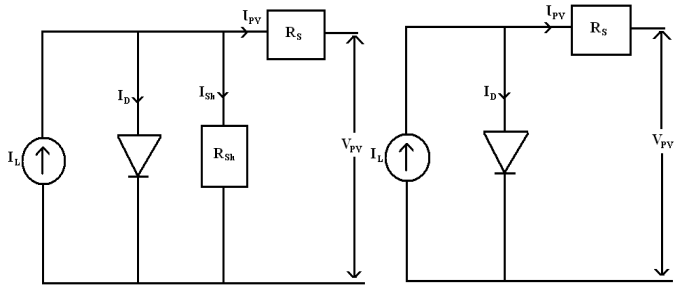

Fig.2. One-diode equivalent circuit models for a PV cell. (a)Five parameters model (b)Simplified four parameters model.

The non-linear curves of V_{pv}-I_{pv} and P-V_{pv} are correspondingly drawn as shown below:

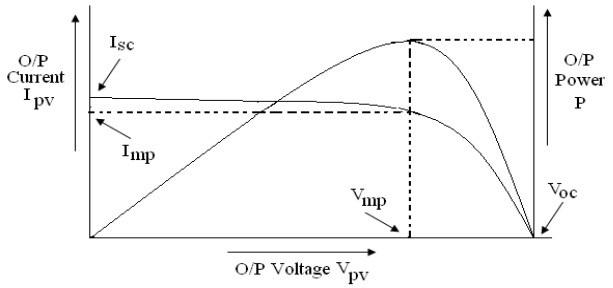

Fig.3. V_{pv}-I_{pv} and P-V_{pv} characteristics of a PV cell

From Fig.(2.b) the relation between the output voltage V_{pv} and the output current I_{pv} can be expressed as:

$$I_{pv} = I_L - I_D = I_L - I_O\left(exp\left(\frac{V_{pv} + I_{pv}R_s}{\alpha}\right) - 1\right) \dots (1)$$

Where I_L = Light current; I_o = Saturation current; R_s= Series Resistance; α = Thermal voltage timing completion factor.
The above four parameters are need to be determined to obtain the V_{pv}-I_{pv} characteristics of PV-module. Thus, this model can be termed as Four-parameter model. The equations for determining the four parameters are as follows:

1. Light Current (I_L)

$$I_L = \frac{G}{G_{ref}}\left(I_{Lref} + \mu_{Isc}(T_c - T_{cref})\right) \dots (2)$$

Where G=solar irradiance (W/m^2); G_{ref} = reference irradiance (1000W/ m^2 is used in this study); I_{Lref} = light current at the reference condition; T_C= PV cell temperature (°C); T_{Cref} = reference cell temperature (25°C is used in this study); μ_{Isc} = temperature coefficient of the short-circuit current (A/°C). From the above equation for light current it can be observed that I_L is a function of both temperature and irradiance.

2. Saturation Current (I_O)

$$I_o = I_{oref}\left(\frac{T_{cref} + 273}{T_c + 273}\right)^3 exp\left(\frac{e_{gap}q}{N_s\alpha_{ref}}\left(1 - \frac{T_{cref} + 273}{T_c + 273}\right)\right) \dots (3)$$

Where I_{oref} = saturation current at the reference condition (Amps); e_{gap} = band gap of the material and is equal to 1.17 eV for Si materials); N_S = number of cells in series of a PV module; q = charge of an electron (1.60217733×10^{-19} C); α_{ref} = the value of α at reference condition.
I_{oref} can be calculated as:

$$I_{oref} = I_{Lref}exp\left(-\frac{V_{ocref}}{\alpha_{ref}}\right) \dots (4)$$

Where V_{ocref} = the open circuit voltage of the PV module at reference condition (V).

3. Calculation of α

$$\alpha = \left(\frac{T_c + 273}{T_{cref} + 273}\right)\alpha_{ref} \dots (5)$$

The value of α_{ref} can be calculated as:

$$\alpha_{ref} = \frac{2V_{mpref} - V_{ocref}}{\frac{I_{scref}}{I_{scref} - I_{mpref}} + ln\left(1 - \frac{I_{mpref}}{I_{scref}}\right)} \dots (6)$$

Where V_{mpref} = maximum power point voltage at the reference condition (V); I_{mpref} = maximum power point current at the reference condition (Amps); I_{scref} = short circuit current at the reference condition (Amps). From the above equation for α, it can be observed that α is a function temperature.

4. Series Resistance (R_S)

If the value of R_s is not provided by the manufacturer, the following equation can be used to estimate its value:

$$R_s = \frac{\alpha_{ref}ln\left(1 - \frac{I_{mpref}}{I_{scref}}\right) + V_{ocref} - V_{mpref}}{I_{mpref}} \dots (7)$$

R_S is taken as a constant in the model of this study.

5. Thermal Model of PV

From equations (1) to (6), it can be noted that the temperature plays an important role in the PV performance. Therefore, it is necessary to have a thermal model for a PV cell/module. In this study, a lumped thermal model is developed for the PV module. The temperature of the PV module varies with surrounding temperature, irradiance, and its output current and voltage, and can be written as:

$$C_{pv}\frac{dT_c}{dt} = K_{inpv}G - \frac{V_{pv}I_{pv}}{A} - K_{loss}(T_c - T_a) \dots (8)$$

C_{PV} = the overall heat capacity per unit area of the PV cell/ module[J/(C-m^2)]; K_{inpv} = Transmittance-absorption product of PV cells ; K_{loss} = overall heat loss coefficient [W/(˚C-m^2)]; T_a = ambient temperature (˚C); A = effective area of the PV cell/module (m^2).

B. Maximum Power Point Tracking of PV Cell Using NEURAL NETWORKS

The block diagram for identifying the optimal operating point using neural networks is shown in Fig.4.

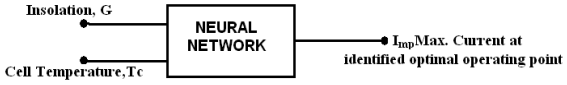

Fig.4. Block Diagram for the identification of optimal operating point

The configuration of 3-layer feed-forward neural network is as shown in Fig.5. The network has 3 layers with 3 neurons in input, 4 neurons in hidden, and 1neuron in output layers [8].

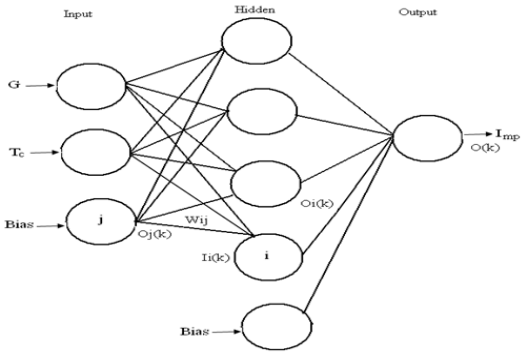

Fig.5. Configuration of a Neural Network

The neuron in the input layer gets input solar irradiance (G) and cell temperature (T_c). These signals are directly passed to the neurons in the hidden layer. The neuron in the output layer provides the identified maximum I_{mp}. For each neuron in the hidden and the output layer, the output $O_i(k)$ is given as follows:

$$O_i(k) = \frac{1}{1 + exp(-I_i(k))} \dots (9)$$

The term Ii(k) is the input signal given to the neuron i at the Kth sampling. The input Ii (k) is given by the weighted sum from the previous nodes as follows:

$$I_i(k) = \sum_j W_{ij}(k) O_j(k) \dots (10)$$

In the above equation, W_{ij} is the connection weight from the neuron j to the neuron i and O_j (k) is the output from neuron j.The process of determining connection weights is referred to as training process[9]-[11]. In the training process, a set of input-output patterns for the neural network is needed. The computations are performed off-line during the training process. With the training patterns, the connection weights W_{ij} recursively until the best fit is achieved for the input-output patterns in the training data. A commonly used approach is the generalized delta rule, where the sum of the squared error described below is minimized during the training process.

$$E = \sum_{k=1}^{N} \big(T(k) - O(k)\big)^2 \dots (11)$$

Where N is the total number of training patterns. T(k) is the target output from the output node and O(k) is the computed one. For all the training patterns, the error function E is evaluated, and the connection weights are updated to minimize the error function E.

C. State Space Model of Boost dc/dc Converter

Solar cells have relatively low conversion efficiency and the improvement of overall system efficiency is an important factor in the area of PV systems. This can be partly achieved by using high efficiency intermediate converters. In this paper, a boost converter coupled with PV array is presented [6]-[7] shown in Fig.6.

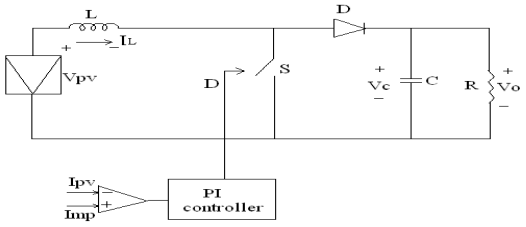

Fig.6 .Circuit Diagram for Boost Converter

The output current I_{pv} and the terminal voltage V_{pv} are measured at a instant and compared with I_{mp} of the neural network. Where I_{mp} is optimal operating point which yields maximum power from PV module. This error is processed through the PI-controller which generates a control signal to shift the operating point I_{pv} and V_{pv} to the optimal operating point.

A state space averaging technique is used to develop linear state space models for dc-dc boost converter. The average state space model for the boost dc/dc converter can then be obtained as follows:

$$\dot{X} = AX + BV_{pv} \dots (12)$$
$$V_o = C^T X \dots (13)$$

Where $X = \begin{bmatrix} I_L \\ V_c \end{bmatrix}$, $A = \begin{bmatrix} 0 & \frac{(1-D)}{L} \\ \frac{1-D}{C} & -\frac{1}{RC} \end{bmatrix}$, $B = \begin{bmatrix} \frac{1}{L} \\ 0 \end{bmatrix}$, $C = [0 \quad 1]$

Where D = Duty ratio of the switch

C. State Space Model of Three-Phase Inverter

A three-phase six-switch PWM VSI is used to convert the power available at the dc bus to ac power. Fig.7 shows the main circuit of the three-phase voltage source inverter connected to the utility grid through the *LC* filter (L_f and C_f) and the coupling inductor (L_s). R_f and R_s in the figure are the parasitic resistances of the filter inductor and the coupling inductor, respectively.

Using the classic electrical circuit theory and state-space averaging technique, a detailed state-space description of the inverter can be obtained [23]-[24].

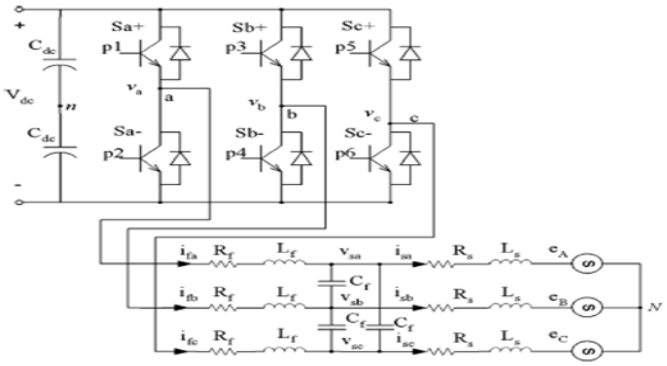

Fig 7: Three phase DC/AC voltage source inverter

IV. CONTROLLER DESIGNS FOR POWER ELECTRONIC DEVICES

In this section, conventional PI-controller is used for the boost dc/dc converters. Also, a *dq* transformed two-loop current control scheme is presented for the space vector pulse width modulation based inverter to control power delivered from the PV cell power system to the grid.

A. Controller Design for the Boost dc/dc Converter

The main components of the dc/dc converter can be determined by the prescribed technical specifications, such as the rated and peak voltage and current, input current ripple, and output voltage ripple, etc., using the classic boost dc/dc converter design procedure [12]-[14]. The component values for the dc/dc converter used in this paper are listed in Table I. Based on the converter model in Fig.6, a PI current controller ($k_{dp} + k_{di}/s$) can be designed using the classic Bode-plot and root-locus method [15].

TABLE- I
PARAMETERS OF THE BOOST dc/dc CONVERTER

Current Ripple(ΔI_L)	0.266A
Voltage Ripple(ΔVc)	0.17777V
Inductance(L)	2mH
Capacitance(C)	150μF
Resistance (equivalent load)	50Ω

B. Controller Design for the Three-Phase VSI

To meet the requirements for interconnecting a PV cell system to a utility grid and control power flow between them, it is necessary to shape and control the inverter output voltage in amplitude, angle, and frequency [17]-[19]. In this section, a space vector PWM controller is designed for the inverter to satisfy voltage regulation as well as to track maximum power. The component values for the three phase inverter used in this paper are listed. The filter inductance and capacitance are L_f =800μH and C_f =400μF, coupling inductance=2mH.The parasitic resistances of the filter inductor and the coupling inductor R_f and R_S are each 5Ω.

The *dq* transformation transfers a stationary (*abc*) system to a rotating (*dq*0) system. The transformation decreases the number of control variables from 3 to 2 (component 0 will be zero) if the system is balanced. Moreover, the *dq* signals can be used to achieve zero tracking error control [24]. Due to these merits, *dq* transformation has been widely used in PWM converter/inverter control and is also applied for the inverter control in this paper as shown in fig. (8).

For accurate current regulation, all AC three phase variables are represented in their d-q vector forms using a reference frame synchronously rotating with the supply voltage. Two PI regulators one for d component the other q component of the current vector are required. The advantage of employing a synchronously rotating reference frame (SRRF) current regulator is well known. The input and the output are DC rather than sinusoidal quantities, hence, enabling the controller to obtain a complete elimination of phase error between the reference and controlled currents at any operating point. The q component of the command current vector is set to zero, while d is defined to be equal to maximum current output of the neural network.

$$V_{ds}^{*} = K_{pc}(I_{ds}^{*} - I_{ds}) + K_{ic}\int(I_{ds}^{*} - I_{ds}) \dots (14)$$

$$V_{qs}^{*} = K_{pc}\left(I_{qs}^{*} - I_{qs}\right) + K_{ic}\int\left(I_{qs}^{*} - I_{qs}\right) \dots (15)$$

where K_{pc} and K_{ic} are the current proportional and integration gains.

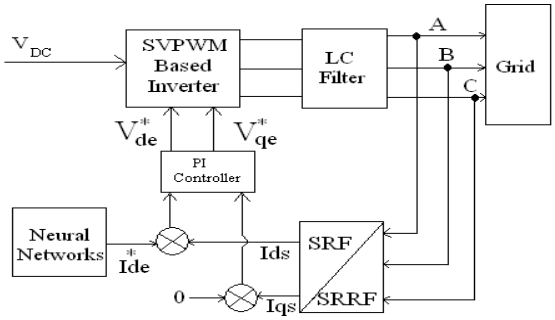

Fig. 8. Block diagram of the overall control system of the inverter

To generate the above calculated voltage vector at the AC side of the inverter, a space vector modulation technique is applied to determine the inverter switching states and their corresponding on-times. In this technique the phase angle of the reference voltage vector, $\bar{V}^{*}$ can be calculated directly using $\bar{V}_{ds}^{*}$and $\bar{V}_{qs}^{*}$. Hence the vector's projection in the d-q plane may lie in the area of one of the six sectors [20,21]. Each sector is edged by two inverter voltage vectors. For a short sampling time interval T_s , $\bar{V}^{*}$ can be regarded as a constant vector Thus, if it is within the area edged by vectors N and N + 1, we can express that as:

$$\bar{V}^{*}T_s = V_N T_N + V_{N+1}T_{N+1} + V_0 T_0 + V_N T_N \dots (16)$$

Where T_N and T_{N+1} are the on-times for vectors V_N and V_{N+1} respectively. T_o is for vectors V_o and T_7 for V_7. To calculate T_N and $T_{N+1}$the modulation index, M is defined as:

$$M = \frac{2\sqrt{2}}{3}\frac{|\bar{V}^{*}|}{V_{dc}} \dots (17)$$

$$\text{Where } |\bar{V}^{*}| = \sqrt{(V_{ds}^{*})^2 + \left(V_{qs}^{*}\right)^2} \dots (18)$$

Subsequently the formulae for the four switching vector on-times are given as:

$$T_N = T_s M sin(60 - \gamma) \ldots (19)$$
$$T_{N+1} = T_s M sin\gamma \ldots (20)$$
$$T_0 = T_7 = \frac{(T_s - T_N - T_{N+1})}{2} \ldots (21)$$

Where γ represents the phase angle of $\bar{V}^*$and T_S is the sampling time. When applying the four switching vectors to control the inverter switches, the switching sequence is defined as $V_O \rightarrow V_N \rightarrow V_{N+1} \rightarrow V_7$. The fundamental component of the inverter output voltage, thus obtained should closely resemble the reference voltage vector $\bar{V}^*$.

V. SIMULATION RESULTS

Based on the mathematical equations discussed before, a dynamic model for a PV module consisting of 153 cells in series has been developed using Matlab/Simulink. The input quantities (solar irradiance G and the ambient temperature T_a) together with manufacturer data are used to calculate the four parameters. Then, based on equation (1), the output voltage is obtained numerically. The thermal model is used to estimate the PV cell temperature. The two output quantities (PV output voltage V_{pv} and the PV cell temperature T_c), and the load current I_{pv}, are fed back to participate in the calculations. The model parameters used in the simulation are given in Table-II

Table II
THE PV MODEL PARAMETERS

$I_{SCref}(I_{Lref})$	2.664A
α_{ref}	5.472
R_S	1.324Ω
V_{OCref}	87.72V
V_{MPref}	70.731V
I_{MPref}	2.448A
G_{ref}	1000w/m^2
T_{cref}	25°c
C_{pv}	5*10^{4}J/(^{0}c-m^2)
A	1.5m^2
K_{inpv}	0.9
K_{loss}	30W/(^{0}c-m^2)

A. Model Performance

The model I_{pv}-V_{pv} characteristic curves under different irradiances are given in Fig.9 at 25˚C. It is noted from the figure that the higher is the irradiance, the larger are the short-circuit current (I_{SC}) and the open-circuit voltage (V_{oc}). And, obviously, the larger will be the maximum power (P), shown in Fig.10.

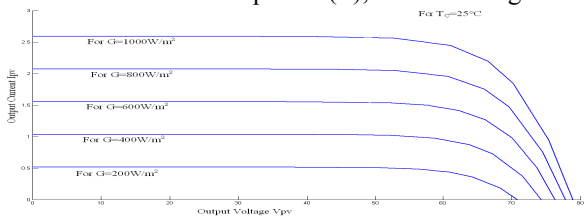

Fig.9 V_{pv}-I_{pv} characteristics for constant T_c and Varying G

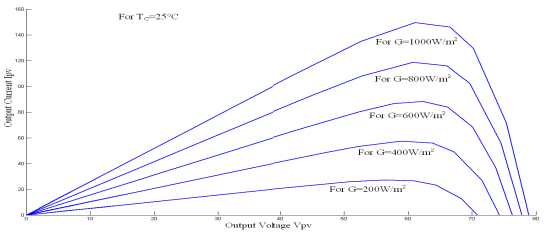

Fig.10. P-V_{pv} characteristics for constant Tc and Varying G

B. Training of a Neural Network

The training of a neural network consists of solar irradiance and cell temperature as the input patterns. The target pattern is given by measured I_{mp} for training the neural network. The I_{mp} is calculated for different values of irradiance and cell temperature w.r.t above modeled PV module. This calculated I_{mp} values are given as a training data to the neural network. Fig.11, shows the convergence of error during training process. During the training process, the convergence error is taken as 0.01.

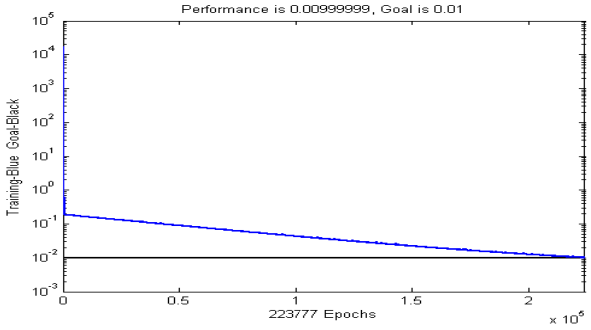

Fig.11. Training of a Neural Network

The graphs for the I_{mp} of the neural network and the calculated values of the PV model, are combined to show the error between the two:

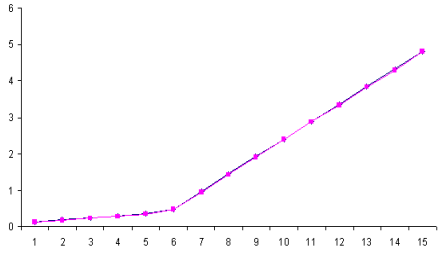

Fig.12. Combined graph of I_{mp} for both neural network and calculated

Note:- The above graphs are drawn for constant T_c=25°c and varying G=50W/m^2-2000W/m^2.

C. Optimal power point tracking for Boost converter and three phase PWM inverter

Comprehensive simulation studies were made to investigate the influence of a boost converter as an intermediate maximum power point tracker for the PV supplied system. As the studies mainly concentrate on maximum power operation of the PV cell, a simulated modeling was developed in the matlab environment, for the PV supplied converter system employing the mathematical models developed in the preceding sections. The

simulated dynamic maximum power point tracking characteristics are shown in Fig's.13&14.

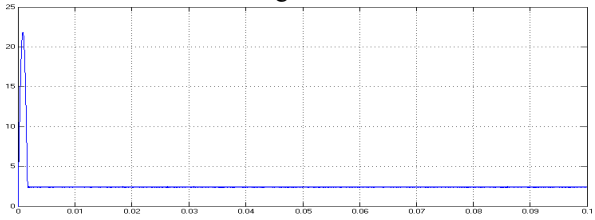

Fig.13. Simulated Dynamic characteristics of inductor current to reach maximum power point

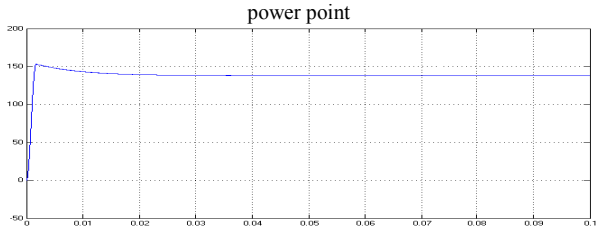

Fig.14. Simulated Dynamic characteristics of capacitor voltage to reach maximum power point

Using the control technique discussed in section-IV for the inverter the simulated waveforms for the Inverter output line-to-line voltage for phase A, inverter output currents, line-to-line voltages and the phase currents across the filter inductor.

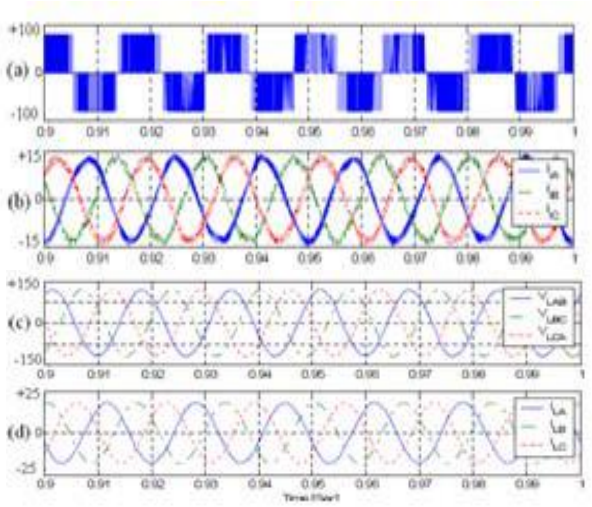

Fig.15. (a) Inverter output line to line voltage
(b) Inverter output current
(c) Load line to line voltage
(d) Load phase current

VI. Conclusion

Modeling, Control, and Simulation study of a GCPV DG system is investigated in this paper. The state space models for the boost dc/dc converter and the three-phase inverter are also discussed. Controller designs for the dc/dc converter and the three-phase inverter are discussed. Conventional PI current feedback controllers are used for the dc/dc converters to regulate the dc bus voltage, and a *dq* transformed two-loop current control scheme is used on the inverter to regulate the voltage and track the maximum power continuously PV cell system to the utility grid. A Matlab/Simulink model of the proposed GCPV DG system was implemented. The validity of the proposed control schemes over a large operating range was verified through simulations on nonlinear converter/inverter models.

References

[1] Cashing Wang "Modeling and Control of Hybrid Wind/Fuel Cell/Distributed Systems", Ph.D Thesis, Montana State University, Bozeman, Montana, July 2006.

[2] Oystein Ullberg, "Stand Alone Power Systems For the future: Optimal Design, Operation & Control of Solar-Hydrogen Systems", Ph.D. Dissertation, Norweigan University of science and technology, Trondheim, 1998.

[3] T.U.Townsend, "A Method for estimating the Long-Term Performance of Direct-coupled Photovoltaic systems', MS Thesis, University of Winsconsin, Madison, 1989.

[4] Smith J.H., and Reiter. L.R, "An In-depth Review of Photovoltaic system performance models, The American Society of Mechanical Engineers,84-WA/Sol-12,1984.

[5] S.M.Alguwainem, 'Matching of a D.C motor to a photovoltaic generator using a step-up converter with a current-locked loop' ,IEEE Transactions on industrial electronics, Vol.9,pp.192-198,Mar.1994.

[6] R.D Middle brook , 'Small-Signal modeling of pulse-width modulated switched-mode power converters', Proceedings of the IEEE, Vol. 76, No.4, pp.343-354, April 1988.

[7] A.Kisiovski, R.Redl, and N.Sokal, 'Dynamic analysis of switching-mode DC/DC converters, New York: Van No strand Reinhold, 1994.

[8] J.G.Kuschewski, 'Application of feed forward neural networks to dynamical system identification and control",IEEE Trans. contr.syst.Tech., vol1,no,1,pp37-49,Mar1993.

[9] J.Lawrence and S.luedeking,"Introduction to Neural Networks", California state software, 1991.

[10] F.Harashima, Y.Demizu, S.Kondo, and H.Hoshimoto, "Application of neural networks to power converters control," in Proc. IEEE ind.Appl. Soc. Annu. Meeting, 1991, pp.415-421.

[11] M.H.Kim, M.G.Simoes, and B.K.Bose,"Neural network based estimation of power electronic waveforms," IEEE Trans.power electron. vol.11, no.2, pp.383-389, Mar.1996.

[12] 'POWER ELECTRONICS - Converters, Applications and Design', Mohan, Under land, Robbins, John Wiley & Sons

[13] 'POWER ELECTRONICS – Circuits, Devices and Applications', Muhammad H. Rashid, Prentice Hall of India Private Limited

[14] 'POWER ELECTRONICS', M D Singh, K B Khanchandani, Tata McGraw – Hill Publishing Company Limited

[15] 'MODERN CONTROL ENGINEERING', Katshuhiko ogata, Printice Hall of India Private Limited.

[16] W. Shireen and M. S. Arefeen, "An utility interactive power electronics interface for alternate/renewable energy systems," *IEEE Trans. EnergyConversion*, vol. 11, no. 3, pp. 643–649, Sep. 1996.

[17] M. Tsai and W. I. Tsai, "Analysis and design of three-phase AC-to-DC converters with high power factor and near-optimum feed forward," *IEEE Trans. Ind. Electron.*, vol. 46, no. 3, pp. 535–543, Jun. 1999.

[18] H. Mao, "Study on three-phase high-input-power-factor PWM-voltage type reversible rectifiers and their control strategies," Ph.D. dissertation, Zhejiang Univ., Hangzhou, Zhejiang, China, 2000. (in Chinese).

[19] *IEEE Standard for Interconnecting Distributed Resources with Electric Power Systems*, IEEE Standard 1547, 2003.

[20] L Zhang, C Wathanasarn, F Hardan, 1994 "An efficient microprocessor-based pulse-width modulator using space vector modulation strategy", IEEE IECON, 9 1-96.

[21] H W VD Broeck, HC Skudelny, G V Stanke, 1988, "Analysis and realisation of a pulse width modulation based on voltage space vector modulation", IEEE Trans Ind, Aual ,*24,* 142-150.